



# STUDY AND IMPLEMENTATION OF AN ATMOSPHERIC PRESSURE PLASMA GENERATOR BASED ON HELICAL COIL

DAN-SEBASTIAN FILIP<sup>1</sup>, DORIN PETREUS<sup>1</sup>

**Key words:** Atmospheric-pressure plasmas, Helical antennas, Finite element analysis, Plasma simulation.

In this paper a free air pressure plasma generator (APPG) is designed and evaluated. The generator is based on quarter wave helical coil in order to obtain the high electric field intensity. After an analytical study, a finite element simulation is constructed in order to better model the electric field around the coil and determine the resonant frequency based on the distributed capacitor formed between the coil and the ground plane. Using the data from simulation, the helical coil is constructed and plasma generation in free air is obtained. Based on practical measurements from the experiment, a simple spice model of the plasma is constructed in order to further improve the system and better understand the plasma properties.

## 1. INTRODUCTION

Plasma is the fourth fundamental state of matter and is characterized simply as an ionized gas. [1] Usually, the plasma is obtained by pumping energy into a neutral gas to the point of which the atoms and molecules collide with each other and break the electric bonds causing the formation of charged particles. [1, 2] There are multiple uses for plasma and based on the field of use, there are a number of ways of producing it. Plasma is used for hydrophilization and hydrophobization, light generation, welding, etc [2] One specific application is in spectrometry, the process of analyzing the free atoms in a substance and evaluate the substance composition. For this application the method of energy infusion and plasma generation is by applying an electric field with high intensity in the neutral gas and start generating plasma.

High intensity electric fields can be generated using helical wound Tesla coils. This approach has the main advantage of generating the plasma at lower input voltage levels than the ones used in arc generators. This also gives the ability of designing a low power portable plasma generator. Analysis of such a system implies understanding field distribution at high frequencies where current distribution inside the coil is not uniform. Considering the helical coil, there is no exact solution for the Maxwell equations. Furthermore, the wave equation is not separable in helical coordinates. [3] In order to overcome this challenge, a finite element model is constructed. This will help in visualizing the electric field distribution and help in the actual design of the helical coil.

In literature extensive research is done regarding the helical antenna with a diameter smaller than the quarter wavelength and radiating pattern normal to the helical coil axis. [4] The analysis is done with respect to transmission lines and antenna design. Optimum matching of the antenna is also described and more than one method is presented [4]

The main idea behind the experiment is to generate a static wave on the coil that reaches the quarter wavelength at the top edge of the coil. This has the advantage of generating a high intensity electric field at the top of the coil by using a coil of relatively small dimensions, approximately a quarter wavelength in height. Because the plasma is intended to be generated in free air, the resonant

tank is established between the inductance of the coil and the distributed air capacitor from the coil to the ground plane. This system will be a high  $Q$  oscillator that will amplify the electric field intensity when the oscillating frequency approaches the resonant frequency.

The mathematical analysis along with the finite elements simulations express the behavior of the system during pre-discharge period, right before actual discharge and plasma generation occurs. The paper includes an analysis of the system load while plasma is generated and addresses the matching impedance network calculation based on practical measurements.

## 2. ANALYTIC SOLUTION

### 2.1. CALCULATING RESONANCE FOR QUARTER WAVE

Starting from the work presented in [3–7] an approximate solution for Maxwell equations for helical coils can be found if the helix is replaced by a cylindrical surface that conducts in the helix direction only. This assumption results in a good approximation that can be used for engineering applications. Considering that the dielectric on both sides of the helical coil have the same properties the velocity factor along the coil axis can be written as

$$V_f^2 = \frac{1}{1 + \left(\frac{M\lambda}{2\pi a}\right)^2}, \quad (1)$$

where  $a$  is the mean radius of the coil,  $\lambda$  is the wavelength and  $M$  is proportional with the helical coil diameter, pitch and frequency. [4] Complex analysis of standing waves for helical antennas with diameters less than free space wavelength give an approximate value for  $M$  as

$$M \approx \frac{20\pi^2 D^5}{(s\lambda)^{2.5}}, \quad (2)$$

where  $s$  is the pitch, and  $D$  is the diameter of the coil. The velocity factor value can then be calculated using the expression as

$$V_f = \frac{1}{\sqrt{1 + 20 \left(\frac{D}{s}\right)^{2.5} \left(\frac{D}{\lambda_0}\right)^{0.5}}}, \quad (3)$$

<sup>1</sup> Applied Electronics Department, Technical University of Cluj-Napoca, Cluj-Napoca, str.G.Baritui, nr. 26-28, Romania, Dan.Filip@ael.utcluj.ro

where  $D$  represents the diameter of the coil and  $s$  is the turns pitch. This approximation gives acceptable results for practical application, with an error of less than 10 %. [3] The approximation is valid if

$$\frac{5nD^2}{\lambda_0} \leq 1, \quad (4)$$

where  $n$  is the number of turns per unit length and  $D$  is the coil diameter. Phase velocity can later be determined as

$$v_p = c \cdot V_f. \quad (5)$$

Based on the phase velocity, the standing wave wavelength can be determined. In order to obtain plasma, the height of the coil needs to be a quarter of the wavelength and can be found simply with

$$l = N \cdot s = \lambda_g = \frac{v_p}{4f_{sw}}, \quad (6)$$

where  $f_{sw}$  represents the oscillating frequency and  $N$  represents the number of turns. It is easy to see that the quarter wavelength depends on the pitch and number of turns of the coil directly and indirectly to the length of the wire used in the coil.

## 2.2. CALCULATING THE COIL DIMENSIONS

The height of the coil and number of turns is critical in obtaining resonance at a specific working frequency. Having a helix, the total length of the copper wire can be determined with

$$L_{wire} = N \cdot \sqrt{4\pi^2 R^2 + s^2}, \quad (7)$$

where  $s$  is the pitch of the coil turns and  $R$  is the radius of the helical coil. Having the geometrical dimensions of the coil, it is possible to calculate the coil inductance using the expression below

$$L_{coil} = \frac{\mu_0 \mu_r \cdot N^2 \cdot \pi \cdot R^2}{l}, \quad (8)$$

where  $N$  represents the number of turns and  $l$  represents the height of the coil. With the resonant frequency found from simulation, the distributed capacitance can be calculated as

$$C_{air} = \sqrt{\frac{1}{4 \cdot \pi^2 \cdot f^2 \cdot L}} \quad (9)$$

where  $f$  is the resonant frequency. This information would give valuable insight of the system parameters and will help at a later stage when adjusting the matching network for maximum power transfer. This capacitance can also be estimated using the empirical formula established by Medhurst through measurements. This is documented in the literature [3] and can be used as a comparison with the results from simulation. Medhurst approximation

$$C_{air} = \left( 0.1126 \frac{l}{D} + 0.08 + \frac{0.27}{\sqrt{\frac{l}{D}}} \right) D, \quad (10)$$

where  $l$  is the height of the coil and  $D$  is the diameter of the coil, both in cm.

## 2.3. DETERMINING THE MATCHING IMPEDANCE NETWORK

The matching network impedance is constructed as a gamma filter topology using two capacitors and an inductor. The general schematic is presented in Fig. 1.

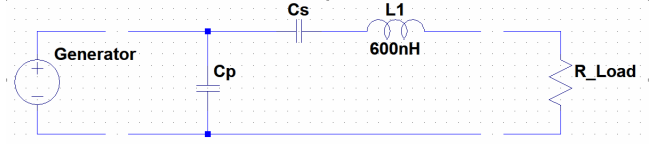


Fig. 1 – Matching network between the generator and load

In order to calculate the values for the two capacitors, it is necessary to know the output resistor of the generator and the plasma resistance. While the generator resistance is specified in the manual, the load resistance is much more difficult to obtain due to gas properties around the plasma. [6] The forward and reflected power from the generator can be used in order to find the load resistance. From here the calculation for the matching impedance network is presented below

$$Q = \sqrt{\frac{R_p}{R_s} - 1}. \quad (11)$$

where  $R_p$  is the source impedance and  $R_s$  is the load impedance for the matching impedance network. The reactance for the filter can be determined with

$$X_s = Q \cdot R_s \quad (12)$$

$$X_p = \frac{R_p}{Q} \quad (13)$$

and, the capacitor value can be calculated

$$C_p = \frac{1}{2 \cdot \pi \cdot f \cdot X_p}, \quad (14)$$

$$C_s = \frac{1}{2 \cdot \pi \cdot f \cdot (2 \cdot \pi \cdot f \cdot L - X_s)}. \quad (15)$$

## 3. FINITE ELEMENT SIMULATION

The usual approach in studying the resonant coils and plasma generation is through mathematical formulas [3]. However, in some cases, visualizing the electric field around the coil can be difficult. With this in mind a finite element simulation environment was proposed. This will give insight into the electric field distribution around the coil for both at resonance and away from it, a good approximation for the test setup and the possibility to change parameters regarding coil dimensions and gas properties around the coil without much difficulty. This simulation will also show the viability of the experiment and test setup, and what are their limitations. The proposed simulation environment is Comsol Multiphysics and it allows to model and simulate the coil in 3D giving a good spatial distribution of the electric field. Using finite element simulation also has its drawback. Because the coil size is

relatively small compared to the ground plane, in order to have a good approximation, the finite element dimension needs to be small compared to the volume it needs to simulate. This adds to the time of finding a solution and completing the simulation. A balance needs to be found between simulation time and result approximation and because of this, in some simulation results, the number of finite elements is low and used just to give a comparison.

### 3.1. MODEL CONSTRUCTION

For the 3D model of the coil the start point is a helix with a major radius of 6 mm and a minor radius of 0.2 mm. That would translate in an air coil with 6 mm in radius and 0.2 mm wire radius. For this wire dimension the minimum pitch for the wire turns is 0.4 mm, but in order to simplify the simulation and not to add a layer of insulation that would add to the simulation time, the pitch was set at 0.5 mm, giving 0.1 mm of air insulation.

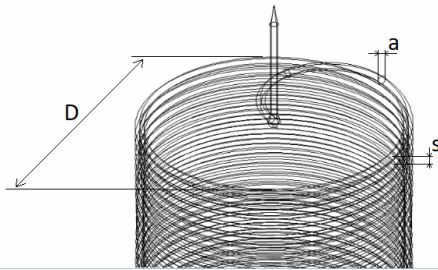


Fig. 2 – Coil termination for generating intense electric fields. The very end is a cone shape to reduce the conductor area and amplify the generated electric field.

On the top of the coil the helix is terminated with a half circle in order to reach the middle of the coil and a vertical cylinder that connects to the half circle and to the coil. This can be seen in Fig. 2. Connection between the half circle and the cylinder is done with a sphere in order to simulate a ball of tin that connects the copper wire of the coil with the tip of the coil made of a different material.

The height of the cylinder is set at 5 mm and it terminates with a cone shape in order to amplify and focus the electric field at the tip of the coil.

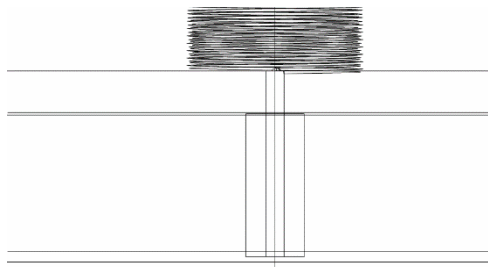


Fig. 3 – Coil feeding point. In the simulation the coil is connected through the metal plane using a pin with PTFE insulation. The bottom part is where the generator will be connected.

At the bottom of the coil a cylinder with a radius of 60 mm and a height of 10 mm is simulating the copper ground plane. The first coil turn is placed at a distance of 3 mm from the ground plane and the connection is done with a circular pin of 0.6 mm in radius through the ground plane. To insulate the pin from the copper plane a cylinder with a radius of 2 mm was placed inside the plane and the insulated material is polytetrafluoroethylene (PTFE), with a

relative permittivity value of 2.1. The generator will be placed on the other side of the copper plane, on the coil pin. This construction is shown in Fig. 3.

The entire system is encapsulated in a sphere with dimension of 100 mm in radius and electric properties of air. In normal situations the sphere is considered infinite but because increasing the dimensions of the simulated models will significantly increase the time for calculating the results, a good approximation is to set the outer layer of this domain to be simulated as perfectly match layer. This will ensure that the generated electric field will not cause reflections when reaching the outer layer of the sphere. The total simulation model can be observed in Fig. 4.

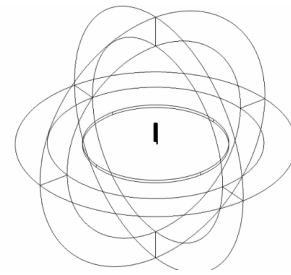


Fig. 4 – Simulation setup. The coil is placed on a large metal plane which is connected to the ground of the frequency generator. For measuring the field around the coil a sphere with air properties encapsulates the entire system.

### 3.2. PHYSICS SIMULATION DOMAIN

In order to simulate the electric field distribution, the preferred physics domain is the “Electromagnetic Wave, Frequency Domain” included in the RF module of the simulation environment. The RF module is used for simulating wave propagation, antenna design and transmission line among other features that are of interest to this simulation. The interest is on the electric field around the coil and therefore it is possible to consider the conductors as a perfect electric conductor. This has the advantage of simulating the surface of the conductor and not inside the conductor, reducing the simulation time [8]. The generator is connected to the pin of the coil situated on the opposite side of the copper plane from the coil. The generator is considered as a coaxial lumped port, as a cable termination type. For simulation the considered voltage is set at 1 V and the characteristic impedance of the terminal is set at 50  $\Omega$ .

The simulation is done in the frequency domain, with parametric sweep in order to simulate at both resonant frequency and away from resonant frequency. The field probe is placed on the tip of the resonant coil using a boundary point probe to evaluate the electric field intensity. Based on the obtained value at different frequency it is possible to determine the resonant frequency. For the mesh parameter the model is constructed with 316048 domain elements, 43922 boundary elements and 15574 edge elements.

## 4. SIMULATION RESULTS

Several simulations were done in order to find the resonant frequency of each coil. The coil number of turns and pitch of the coil turns were changed in order to have an

optimum coil design. Because the generator is set at 27.12 MHz generated frequency, due to legislation constraints, this value is the target for the resonant frequency of the coil.

For a coil with 133 turns and 0.5 mm turn pitch, the simulation shows a resonant frequency of 28 MHz, close to the intended target. Because the simulation includes geometrical shapes that have large and small dimensions, there needs to be a significant number of finite elements in order to have a usable result. This translates in a long simulation time. The accepted compromise was to reduce the number of frequency points simulated when finding the resonant frequency. This can be observed in the Fig. 5.

Because the number of computed frequencies is low, we cannot say with certainty the exact resonant frequency value, however, this is not critical as the physical coil will have tolerances that will influence the resonant frequency value. Having the coil resonant frequency in the vicinity of the intended resonant frequency is sufficient. For finding the resonant frequency, the electric field intensity was measured at the top of the coil, knowing that for the resonant frequency the value will increase dramatically.

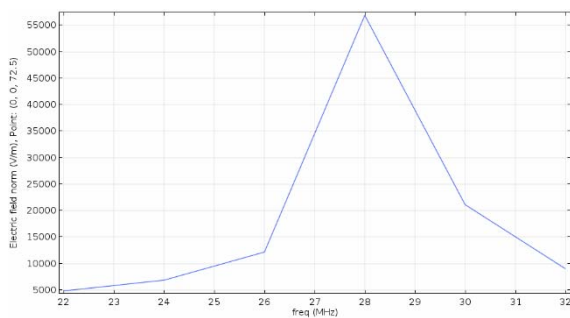


Fig. 5 – Point probe measurement of the electric field on the top side of the coil with respect to frequency. This shows the resonant frequency to be around 27 MHz

One of the advantages of using finite element simulation is the possibility of showing the electric field intensity around the coil. In Fig. 6 is a color representation of the electric field intensity when the coil is close to resonance, at 28 MHz. The field is more intense at the top of the coil, reaching its maximum value at the end point of the coil. This is where the cone shape end of the coil becomes significant as it concentrates all the field on a small surface and plasma generation is obtained. In the simulation, the generator gives a voltage amplitude of 1 V. On the top of the coil the simulated value for the field intensity reaches 55 kV/m. In reality, this value will be lower, because after generating the plasma, the behavior of the circuit will change. Due to time and analysis constraints, the plasma properties are not included in the simulation and therefore the discharge is not triggered, allowing the field intensity to increase significantly above normal situation.

Another interesting observation is the electric field intensity at the bottom of the coil, close to the ground plane. At resonant frequency the propagation has the wavelength equal to 4 times the height of the coil. In other words, reaching the maximum intensity on the top of the coil leaves the bottom of the coil to have the minimum of the field intensity. This is also easily observed in Fig. 6.

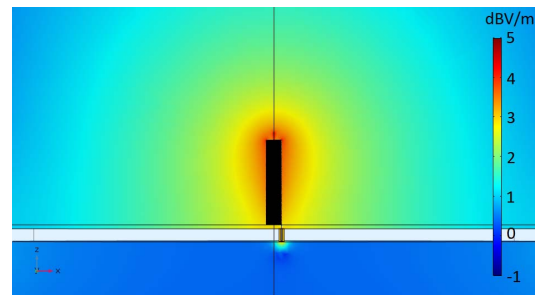


Fig. 6 – Logarithmic representation of the electric field distribution for the plasma coil close to resonant frequency. The field is at its peak in the tip of the coil and radiates towards the ground plane. This is measured at 28 MHz, close to the resonant point.

Looking close to the coil, the field intensity drops from the top of the coil towards the bottom. Notice that farther from the coil, the field distribution depends on the distance from the coil and not the height of the coil.

For comparison, in Fig. 7 is presented the electric field intensity when the generator frequency is higher than the resonant frequency. The electric field intensity on the top of the coil is much lower than in the case of the resonant frequency. This is also because the height of the coil is larger than the quarter wave length of the propagation frequency.

The minimum intensity of the field can be observed at a distance from the ground plane, after a few turns of the coil. This is also an indication that the coil is not driven at the resonant frequency, and optimum design is not obtained. On a more practical note, in this situation plasma generation can also be obtained if enough power is injected into the coil, however the efficiency will be reduced and thermal issues can appear due to higher losses in the coil.

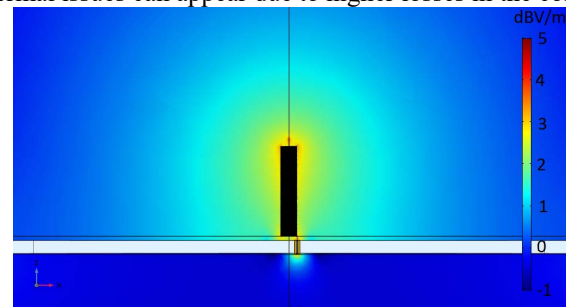


Fig. 7 – Logarithmic representation of the electric field distribution for the plasma coil at 32 MHz. The field is at its peak in the tip of the coil and radiates towards the ground plane. The field intensity is lower compared to the resonant frequency measurement and notice that the minimum field on the surface of the coil is reached above the first coil turn.

A few other dimensions of the coil were simulated in order to verify the simulation accuracy and also to check if other combinations of number of turns and turn pitch can be used. As expected the changes in coil construction influenced the resonant frequency of the coil. The simulation results are presented in the Table 1.

Based on the formulas (3), (5) and (6) presented earlier it is possible to calculate the resonant frequency of the coil. The calculations were done in Mathcad for each coil dimension that was simulated and the results are presented in Table 1. Due to simulation time constraints there is a sampling error between calculated results and simulated results. However, even with this variation the error is kept

well below 10 % indicating that the simulation model is in close approximation with the theory.

Table 1  
Measurement values and comparison

| Number of turns N | Pitch s | Coil height l | Simulated resonant frequency | Calculated resonant frequency | Relative error |
|-------------------|---------|---------------|------------------------------|-------------------------------|----------------|
| [ ]               | [mm]    | [mm]          | [MHz]                        | [MHz]                         | [%]            |
| 30                | 0.5     | 15            | 86                           | 86.7                          | 0.80738        |
| 60                | 0.5     | 30            | 53                           | 49.9                          | -6.2124        |
| 133               | 0.5     | 66            | 27                           | 26.4                          | -2.2727        |
| 60                | 1.2     | 72            | 63                           | 59.4                          | -6.0606        |
| 60                | 2.4     | 144           | 69                           | 67.7                          | -1.9202        |

The preferred working frequency is 27.12 MHz as this frequency window is reserved for research and approved by country legislation. Therefore, based on the results we obtained, the 133 turns coil is the intended target for experimental data. To better visualize the influence of turns pitch of the coil on the target resonant frequency, a plot is presented that shows the height of the coil as a function of turn pitch and the quarter wave length for a 133 turns coil as a function of turn pitch. Notice that the two functions intersect at the 0.5 mm pitch mark.

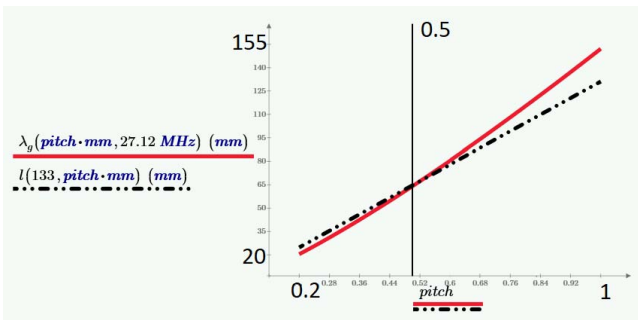


Fig. 8 – Variation of the quarter wave length resonant frequency with respect to turn pitch versus height of coil with respect to turn pitch.

Small variations in the turn pitch of the coil will not significantly change the quarter wave length. Additionally, it is possible to slightly change the number of turns and still be close to resonant. This can also be used when changing the coil diameter and help in finding a resonant frequency based on height restrictions. With this information the next step was the construction of the coil and experimental tests to verify the calculated and simulated results.

## 5. EXPERIMENTAL RESULTS

A coil with 133 turns was constructed on a Teflon tube in order to generate the plasma. The copper wire has a diameter of 0.4 mm to which an 0.1 mm insulation is added giving a total diameter of 0.5 mm, in order to easily obtain the 0.5 mm pitch of the turns. The diameter of the coil was 12 mm and the height of the coil was 66.5 mm. Additionally 3 mm of Teflon tube was left at the bottom of the coil in order to have a distance from the ground plane. On the top of the coil a thin rod of tungsten was placed in order to obtain the cone shape at the tip of the coil. This

material has the property of self-sharpening while generating the plasma.

The used generator is the CESAR 273 RF generator. The output resistance is set at 50  $\Omega$  and generated output frequency is fixed at 27.12 MHz. Maximum output power is limited at 300 W, however the experiment aims for a minimum power requirement. The generator also measures the reflected power and through this gives a feedback on network matching and delivered power.

The Navi Digital Matching Network is used for network matching between the RF generator and the resonant coil. The network consists of two variable capacitors having maximum capacity of  $C_s = 310$  pF and  $C_p = 800$  pF and a coil of fixed value of 600 nH. The circuit topology is a L matching network and is presented in Fig. 1. In order to calculate the capacitor values it is required to know the equivalent load resistance, the resistance of the plasma. Because the plasma resistance depends on atmospheric factors it is difficult to estimate the resistance. A different approach is used in which the reflected power is measured and the matching impedance is adjusted in order minimize this reflected power.

The plasma is generated at the top of the coil and the measured input power is set at 40 W. By adjusting the two variable capacitors for the matching impedance network, the measured reflected power is reduced to 0 W translating into impedance matched. This means that all the power from the generator is concentrated in the plasma. The plasma, coil and generator can be seen in Fig. 9 and the output power versus reflected power measured by the generator is seen in Fig. 10.

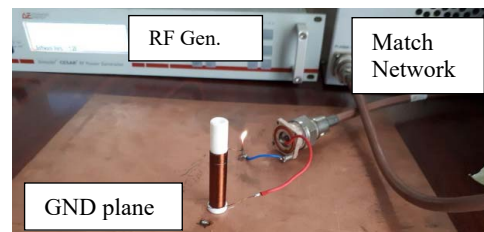


Fig. 9 – Plasma generation using a resonant coil. The resonant coil is connected to a generator of 27.12 MHz through a matching impedance network in order to eliminate the reflected power and increase efficiency.



Fig. 10 – The generator is set at 39 W of output power and the matching impedance is adjusted in order to obtain 0 W reflected power.

Considering the maximum variable capacitors values from the matching impedance network, 310 pF and 800 pF and the percent adjustment from the generator, seen in Fig. 10, the final capacitors value are set at  $C_p = 269.6$  pF and  $C_s = 43.09$  pF. Using the relations presented earlier, it is possible to calculate, with some approximation, the resistance of the plasma and based on this value, and the power supplied by the generator, it is possible to estimate the voltage at the tip of the coil. This is the value obtained in the atmospheric conditions present in the lab at the time of the tests.

When calculating the capacitor values for the matching network using (11-15),  $C_p = 269.6$  pF and  $C_s = 69.939$  pF and the plasma resistance is estimated at  $8 \Omega$ . At first glance the value for the series capacitance is far from the set value, however, the value was calculated without considering the parasitic components of the coil which can add to the series capacitance. Considering all the determined values, it is possible to construct an equivalent circuit in LTSpice in order to simulate the plasma. The circuit is presented in Fig. 11.

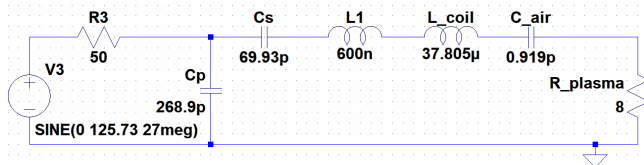


Fig. 11 – Plasma generator equivalent circuit. The circuit includes the generator output resistance, matching impedance network with the calculated capacitors values, coil inductance, estimated distributed air capacitance and resistance of the plasma.

The generator is modeled as a simple sine wave voltage source with peak amplitude of 125.73 V and an output impedance of  $50 \Omega$ . The amplitude was chosen based on measurements taken from the generator after successful plasma generation. The matching impedance capacitors values are the values computed, as the coil parasitic capacitance is not included in the simulation. For the distributed air capacitance from the tip of the coil towards the ground plane, the Medhurst approximation was considered. The plasma resistance is set at  $8 \Omega$ .

At this point it is possible to check for resonance by measuring the current through the coil and the voltage at the bottom of the coil. In the simulated circuit, this is the connection point between the  $L_{coil}$  and the output of the matching circuit,  $L1$ . For resonance the current and voltage need to be in phase, and this can be verified in Fig. 12.

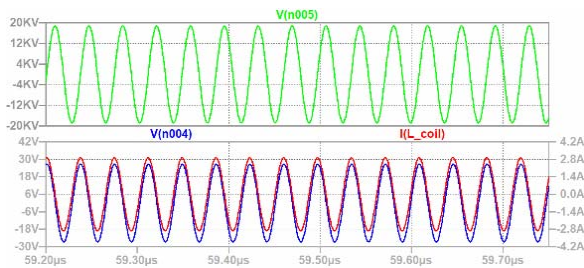


Fig. 12 – Waveforms on the simulated equivalent circuit. Top waveform is the voltage at the plasma generating edge of the coil. Bottom waveforms are the voltage at the bottom of the coil, where it connects to the matching network and the current through the coil. These are in phase confirming resonance.

The output power from the generator is measured at 39.142 W and is also evaluated in the simulation at the connection point of  $C_p$ ,  $C_s$  and  $R_3$ . The power computed on the  $R_{plasma}$  resistor is 34.38 W. As expected, the rest of the power is through the coil, and is evaluated at 4.61 W. Through the simulation it is possible to estimate the peak voltage on the edge of the coil, at the tip where the plasma is generated. The peak voltage reached at the top of the coil is close to 19 kV, enough to ionize the air around it and generate plasma.

## 6. RESULT INTERPRETATION

The finite element simulations show the electric field around the coil and is a good estimation of the resonant frequency of the coil. It is also possible to evaluate the field value in different points around the coil, for example on the edge of the last turn, or inside the center of the coil. Because of performance and time constraints of the simulation the finite element and number of simulation points was kept at a level where the simulation results are acceptable compared with the time it takes for solving it. The simulation does not take into account the generation of plasma at the end of the coil. For this a new domain had to be added to the simulation and this would have the downside of longer simulation times.

Not adding the plasma domain means that the simulation only evaluates the phenomenon just before air ionization occurs. Since this will not be modeled, the simulation shows electric field higher than 55 kV/m at the top of the coil Fig. 5. Naturally, in case of the experiment in the lab, the discharge will appear at a lower field intensity and plasma generation will begin. This can be observed when comparing the finite element simulation with the constructed LTSpice model. The LTSpice model includes the resistance value of the load, estimated after real measurements and for this, the measured voltage at the plasma generation end of the coil reaches 20 kV, a much lower value than in the case of the finite element simulation.

Considering that in dry air, the necessary electric field intensity in order to create a discharge is estimated at 3000 V/m, we can safely assume that even with a reduced output power it is possible to obtain plasma using the same coil. The air properties around the coil at the moment of generating plasma are important in power consumption, and translate in a change in resistance value of the plasma, it is possible to estimate a minimum power in order to obtain the plasma.

From the top of the coil towards the ground plane, it is possible to consider a distributed capacitor that plays an important role in the formation of the resonant tank and is important in fine tuning the resonant frequency. The capacitance depends on the air properties surrounding the coil, and in turn, the plasma generation is dependent of it. Having other materials around the coil can influence the plasma. For this situation the finite element simulation can also help, by changing the properties of the air around the coil. Comparing the simulation with the calculated results, when constructing the coil in order to obtain resonance at a specific frequency, it is important to find a pair of number of turns and turn pitch in order to get the best result.

## 7. CONCLUSIONS

Starting from a mathematical approach and followed by finite element simulation, plasma generation was managed in free air by using a helical coil. While the mathematical approach uses approximations in order to find the solution, the finite element simulation gave a more practical visualization of the experiment and provided with insights on coil resonance through free air. Based on the results from

both equation solutions and simulation the coil was constructed and plasma was generated in free air.

The practical measurements from the experiment gave more insight into plasma generation and plasma properties allowing the possibility to construct a simple LTSpice model and help in adjusting the matching impedance network and measure the peak voltage amplitude at the top of the helical coil.

The experiment is a proof of concept on a system that can generate plasma in free air at approximately 40 W power. Further test can be conducted in order to improve the efficiency and further reduce the dimensions of the coil, based on the working frequency.

*Received on February 21, 2019*

## REFERENCES

1. R. J. Goldston, P. H. Rutherford, *Introduction to Plasma Physics*, Plasma Physics Laboratory Princeton University.
2. H. Conrads, M. Schmidt, *Plasma generation and plasma sources*, INP Greifswald, Institut für Niedertemperatur-Plasmaphysik e.V., "Friedrich Ludwig-Jahn-Str. 19, D-17489 Greifswald, Germany.
3. K.L. Corum, J.F. Corum, *RF Coils, Helical Resonators and Voltage Magnification by Coherent Spatial Modes* TELSIS 2001, University of Nis, Yugoslavia, September 19-21, 2001.
4. A.G. Kandoian, W. Sichak, *Wide-Frequency-Range Tuned Helical Antennas and Circuits*, Federal Telecommunication Laboratories, Inc. Nutley, New Jersey.
5. W. Sichak, *Coaxial Line with Helical Inner Conductor*, Proceedings of the I.R.E., pp 1315-1319, Menasha, USA, September, 1954.
6. D. Petreus, A. Grama, S. Cadar, E. Plaian, A. Rusu, *Design of a plasma generator based on E power amplifier and impedance matching*, Optimization of Electrical and Electronic Equipment (OPTIM), 2010.
7. A. Ganguli, P. Appala Naidu, D.P. Tewari, *Studies on Microwave-Induced Plasma Production Using Helical Slow-Wave Structures*, IEEE Transactions on Plasma Science, **19**, **2**, April 1991.
8. *Two-Arm Helical Antenna*, Comsol Tutorial.